Measurements of urea and glucose in aqueous solutions with dual-beam near-infrared Fourier transform spectroscopy

Snoer Jensen, Peter; Bak, Jimmy

Published in:
Applied Spectroscopy

DOI:
10.1366/000370202321115869

2002

Measurements of Urea and Glucose in Aqueous Solutions with Dual-Beam Near-Infrared Fourier Transform Spectroscopy

PETER SNOER JENSEN* and JIMMY BAK

Risø National Laboratory, Optics and Fluid Dynamics Dept., Denmark (P.S.J., J.B.); and Lund Institute of Technology, Dept. of Physics, Sweden (P.S.J.)

This study investigates the use of a dual-beam, optical null, FT-IR spectrometer to measure trace organic components in aqueous solutions in the combination band region 5000–4000 cm^{-1}. The spectrometer may be used for both single- and dual-beam measurements, thereby facilitating comparison of these two modes of operation. The concentrations of aqueous solutions of urea and glucose in the ranges 0–40 mg/dL and 0–250 mg/dL, respectively, were determined by principal component regression using both modes. The dual-beam technique eliminated instrumental variations present in the single-beam measurements that must be taken into account when quantifying trace components from single-beam spectra. The data obtained with the dual-beam technique resulted in more stable calibration models based on principal component regression. These calibration models need fewer factors and yield lower prediction errors than those based on traditional single-beam data.

Index Headings: **Near-infrared; FT-IR; Dual-beam; Optical null; Optical subtraction; Aqueous solutions; Glucose; Urea.**

INTRODUCTION

The quantification of trace organic components in aqueous solutions by near-infrared transmission spectroscopy is important in a number of widely different applications within the dairy food industry and medical diagnostics.[1–9] In traditional FT-(N)IR spectroscopy a single-beam spectrum of the solution is measured. The dominant features of such a spectrum are the water absorption and the source characteristics. The signals from the trace components are much smaller and are therefore difficult to separate from the water absorption. Usually a reference measurement is used to remove variations caused by changing water absorption and instrument conditions. This approach is successful only if the reference is constant and instrumental conditions do not change between the measurement of the reference and of the sample. The temporal separation of the two measurements is problematic because instrument variations may easily be comparable in magnitude to the signals from the trace components of interest. Chemometric calibration methods, such as principal component regression (PCR) or partial least squares (PLS), must build such variations into the calibration model to accurately determine the solute concentration. The accuracy and stability of the calibration will be lower in the presence of instrumental variations.

This paper demonstrates that the quality of measurements can be improved by using a dual-beam technique in which the water absorption and source characteristics are removed by simultaneous measurement of the difference between the sample and the reference. This technique has a number of different implementations and is known by a variety of names, including dual-beam, double-beam, optical nulling, and optical subtraction. In our study, light was sent through a reference cell containing pure water and through a sample cell and entered the spectrometer through two different emission ports. The sum of the two signals was then measured on one detector after leaving the interferometer. This is known as a double-input–single-output configuration. The term ''optical subtraction'', used by Griffiths and de Haseth,[10] is perhaps the most appropriate name for this mode of operation. It refers to the simultaneous, out-of-phase interference on the detector of the reference and sample signals. The term ''optical subtraction'' distinguishes this technique from other dual-beam techniques, such as the one employed in traditional grating instruments and techniques employing two detectors. Nevertheless, we shall use the shorter term ''dual-beam'' for the optical subtraction mode of operation and the term ''single-beam'' for the normal mode of operation of the FT-IR instrument. Dual-beam techniques have previously been used with some success in the mid-IR for a number of different applications: detection of anisole in gas chromatography (GC) FT-IR;[11–14] detection of polyester fibers;[15] emission spectroscopy; [16–18] detection of adsorbed polymer monolayers on mica;[19–20] studies of Bacteriorhodopsin in membranes;[21] and gas analysis.[22] A review of the subject prior to 1986 is given by Griffiths and de Haseth.[10] These applications have been limited by the nonlinear behavior of the mercury cadmium telluride (MCT) detector used in the mid-IR. The dual-beam technique should be much more applicable in the near-infrared, where linear detectors such as InAs or InSb are available. Further advantages in the near-infrared spectral region are that the beam splitter does not absorb in the near-IR and that thermal radiation from the samples is small. For measurements of aqueous solutions, optical alignment and the nulling of the two input signals are facilitated by the low spectral resolution required and the usable spectral range, which is limited by the absorption of water for any fixed choice of pathlength. Finally, more intense sources of light are available in the near-IR and may be employed with greater advantage with dual-beam techniques.

Motivated by future applications within the biomedical field, such as quantitative analysis of minor components in body fluids and hemodialysis fluids, we are engaged in a search for sensitive and stable infrared spectroscopic methods. We have constructed a dual-beam FT-IR instru-

Received 17 June 2002; accepted 13 August 2002.
* Author to whom correspondence should be sent.

0003-7028/02/5612-1593$2.00/0

ment and have tested it on aqueous solutions in the near-infrared spectral range. In this paper we present an experimental comparison of the dual-beam technique and the traditional single-beam technique for determining trace components in aqueous solutions. Trace component combination band signals from urea and glucose in the spectral region 5000–4000 cm^{-1} were measured by the dual- and single-beam techniques. The two types of measurements were taken on the same samples with little time separation, enabling direct comparison of the data quality in the two modes of operation. The comparison shows that the dual-beam technique eliminates the water absorption and source characteristics, with the result that only the trace component signal is measured and digitized. The dual-beam technique also reduces the influence of instrumental variations. By calibration using principal component regression, the dual-beam technique provides calibration models with fewer principal components that yield more accurate and stable results than those obtained with the single-beam technique.

EXPERIMENTAL

Instrument Description. The dual-beam instrument consists of a Bomem MB155 FT-IR spectrometer with corner cubes and a KCl beam splitter. The spectrometer has two emission ports with ZnSe windows, and is equipped with a Peltier cooled InAs detector. The wavenumber region is restricted to 5000–4000 cm^{-1} by an optical long-wave pass filter (LP-2000, Spectrogon AB, Sweden) placed in the sample compartment of the spectrometer. This filter removes the near-infrared part of the spectrum while water absorption and detector sensitivity exclude the mid-infrared part. The spectrometer is operated through a Windows NT 4.0 (Microsoft Corp.) PC with installed Grams/32AI Version 6 (Galactic Industries Corp.). The spectrometer is equipped with an external 150 W quartz-halogen light source. The light from the external source is collected by two identical off-axis paraboloidal gold mirrors with 90° deflection (Janos Tech.), with effective focal lengths f_1 = 50.6 mm, and sent through two liquid transmission cells. The light is then collected and collimated by two identical off-axis paraboloidal mirrors with focal lengths f_2 = 108.4 mm (Janos Tech.) and sent into the spectrometer through the two emission ports. Two diaphragms are placed before the transmission cells to regulate the intensity of the two beams. A schematic drawing of the instrumentation is shown in Fig. 1. One transmission cell is filled with pure water and works as a reference; the other is filled with the sample solution. The spectrometer may be used in single-beam mode by blocking the input from the reference cell and in dual-beam mode by using both inputs. To monitor the reference cell alone, the input from the sample cell may also be blocked. The amplification of the detector signal to be digitized may be adjusted through a hole in the housing of the detector. The optical layout is similar to that used by Tripp and Hair[20] for mid-IR measurements of adsorbed polymers on mica. The main difference is that we use a common source for the two input beams instead of two separate sources. The transmission cells are variable pathlength transmission cells (Specac 7000, 7005) with ZnSe windows that may be adjusted by turning one window mounted on a screw

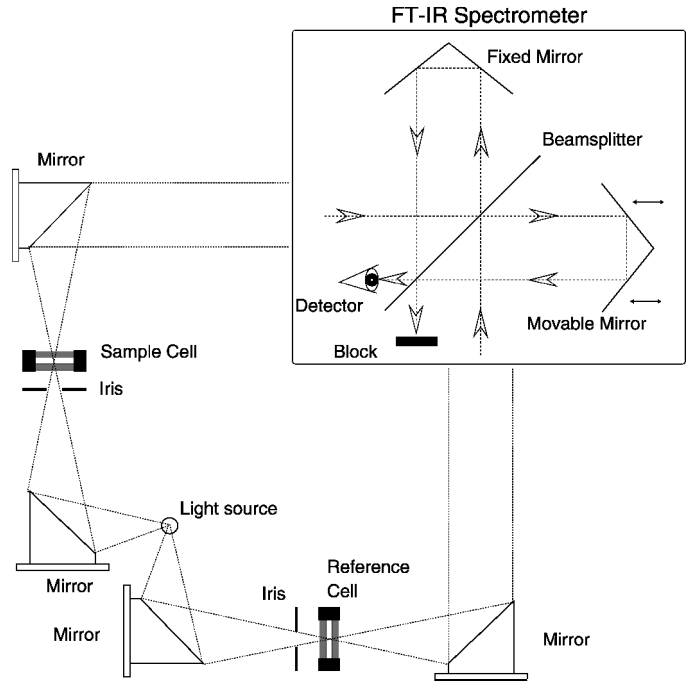

FIG. 1. Diagram of experiment.

thread. The reference cell is calibrated by the fringe method and the pathlength adjusted to 1.00 mm. The sample cell is matched to the reference cell by adjusting it to obtain 100% transmittance of the water-filled sample cell relative to the water-filled reference cell. Both transmission cells were thermostated to 32 ± 0.02 °C by a Eurotherm 4208 control unit that measured sample temperature through the cell-filling port with a PT100 thermo element and heated the cell by a nichrome wire wound around the cell body. The instrument configuration has been optimized for measurement of single-beam interferograms. Center burst intensities have an amplitude of 3.5 V at the lowest amplification to keep within the analog-to-digital converter (ADC) range of ±4 V. Consequently the single-beam measurement cannot be further optimized by increasing the source intensity. An important feature of this system is the ability to measure both single- and dual-beam spectra of the same sample without changing the instrument or the sample. To switch from single-beam to dual-beam measurement, one simply removes the block from the reference arm and increases the amplification of the detector signal to the maximum (15 times the minimum) to fill out the ADC with the smaller dual-beam signal. This change takes less than 10 s.

Reagents. Solutions were prepared by weighing the solute, which was dried reagent grade D-glucose (BDH Laboratory Supplies, Poole, England) or urea (Merck), and dissolving it in 0.5 L water. The concentration uncertainty is determined by the accuracy of the analytical balance and is estimated to be ±0.1 mg/dL.

Measurements. Double-sided (symmetrical) interferograms which contained 2048 points were measured at 32 cm^{-1} resolution with 128 coadditions. The reference cell was filled with pure water and thermostated to 32 ± 0.02 °C. For each sample, the sample cell was filled with sample solution, after which the temperature was allowed to stabilize for approximately 45 min to 32 ± 0.02 °C.

Three different measurements were taken: a single-beam measurement of the sample (reference arm blocked) with lowest amplification; a single-beam measurement of the reference (sample arm blocked) with lowest amplification; and a dual-beam measurement of the sample (both inputs used) with highest amplification. The single-beam and dual-beam measurements of the sample were carried out in random order in all data sets. Each measurement was taken three times. The total measurement time for each sample was about 5 min. We thus obtained a dual-beam and a single-beam data set, with little separation in time between the two types of measurements compared to the time taken to stabilize the temperature of the sample. The single-beam measurements of the reference were not used for data analysis, but were carried out for diagnostic purposes should any anomaly occur. A calibration data set was taken on one day and an independent test set was measured between 1 and 3 days later. No samples from the calibration set were included in the test. Samples were selected at random to eliminate any chance correlation between sample concentration and instrumental drifts. Urea samples were in the concentration range 0–40 mg/dL. There were 11 samples in the calibration set (giving 33 measured spectra). The number of samples in the test set was 9 (27 measured spectra). Glucose samples were in the concentration range 0–250 mg/dL. There were 7 samples in the calibration set (21 measured spectra). The number of samples in the test set was 8 (24 measured spectra). As sample variability is low, few samples were required to model the sample variation. The repeated measurements on the same samples ensured that instrument variations were well represented in the data sets.

Data Analysis. Spectra were transferred from the Windows NT 4.0 (Microsoft Corp.) PC to an Intel PII-based Linux workstation for further analysis. All data analysis was carried out with ANSI C programs using double precision versions of subroutines from Numerical Recipes in C.[23] The interferograms were transformed to intensity spectra by the following procedure. A best-fit straight line through the endpoints (5% of the total data in each end) of the interferogram was calculated and subsequently subtracted to remove any offset and tilt. The interferograms were then apodized by a cosine window and zero-filled by a factor of eight. The phase spectrum, $\Phi(\bar{\nu})$, was calculated as $(\Phi(\bar{\nu})) = \text{atan}(\text{Im}(\bar{\nu})/\text{Re}(\bar{\nu}))$, where $\bar{\nu}$ is wavenumber, and Re and Im are the real and imaginary parts of the Fourier transform of the interferogram, respectively. The intensity spectrum, $I(\bar{\nu})$, were then calculated as $I(\bar{\nu}) = \text{Re}(\bar{\nu}) \cos(\Phi(\bar{\nu})) + \text{Im}(\bar{\nu}) \sin(\Phi(\bar{\nu}))$. For dual-beam spectra, the phase spectrum from a stored pure water single-beam spectrum was used to construct the intensity spectrum because the phase determined from a dual-beam spectrum is poorly defined. The low resolution of the spectrum results in leakage of information from neighboring data points. This is not a problem with a single-beam spectrum where neighboring points have nearly identical and positive intensity. For a dual-beam spectrum, however, the neighboring points may be either positive or negative, resulting in a phase change of π under the usual assumption that intensity is positive. This assumption does not hold for differential spectra, where leakage means that the phase may change in an uncontrolled manner since it will be a linear combination of the phase of the neighboring points.[24] The intensity spectra were restricted to the wavenumber range 5000–4000 cm^{-1}, thereby reducing them to 519 data points each. Identical data analyses were carried out on single-beam and dual-beam data. Intensity spectra were mean-centered and principal component regression was carried out. No outliers were removed, and no preprocessing of spectra was carried out. A few spectra are presented as second-derivative spectra. These were calculated by finite three-point centered differencing as $d^2I_i/d\bar{\nu}_i^2 = (I_{i+1} - 2I_i + I_{i-1})/2$; where I_i is the spectrum and the index i refers to a given wavenumber point.

THEORY

As described in the Experimental section, the spectrometer works in what is known as double-input–single-output mode, where light is passed through the sample and the reference before entering the interferometer and the output from one of the output ports is sent to the detector. One beam emerges from the beam splitter as the sum of the light from the arm that has undergone two reflections and from the other arm that has undergone two transmissions. The other beam to emerge from the beam splitter is the sum of the light from two arms, each of which has undergone one reflection and one transmission. The net result is a phase difference of π between the two signals such that an identical sample and reference result in a zero signal at the detector where the two signals are combined. The double-input–single-output setup requires that the light sources for the two inputs have identical characteristics. We achieved this by collecting the light for both inputs from one source. The general theory for dual-beam spectroscopy with two inputs and two outputs is given by Genzel, Chandrasekhar, and Kuhl,[25] from which we extract the results below. Assume two monochromatic sources, at wavenumber $\bar{\nu}$, with intensities p_1 and p_2. The intensity at the detector, P_1, as a function of the phase shift $\varphi = 2\pi\bar{\nu}\gamma$, introduced by the optical path difference γ, between the two arms of the interferometer, is then given by:

$$\begin{aligned} P_1 = {} & p_1 2RT(1 + \cos\varphi) \\ & + p_2[(R + T)^2 - 2RT(1 + \cos\varphi) \\ & \quad + 4RT\cos\Phi\cos(\varphi - \Phi)] \\ & + 4(p_1p_2RT)^{1/2}\cos(\varphi/2) \\ & \times [R\cos(\Phi - \delta - \varphi/2) + T\cos(\Phi + \delta - \varphi/2)] \end{aligned} \tag{1}$$

where R and T are the beam splitter reflectance and transmittance, respectively, Φ is the phase difference between the reflected and transmitted beams on the beam splitter, and δ is the phase difference between the two input channels. If the two inputs are uncorrelated, the last term will vary rapidly and average to zero on the detector. When collecting light from the same source, this condition may not always be met. To avoid this effect, we collect the light at right angles from the same source and from a large area. We collect the light from one source only to ensure that any source drift will be of the same nature in

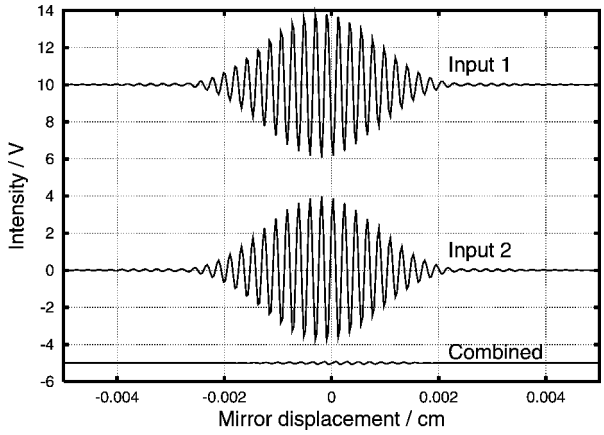

FIG. 2. Interferogram, anti-interferogram, and dual-beam interferogram.

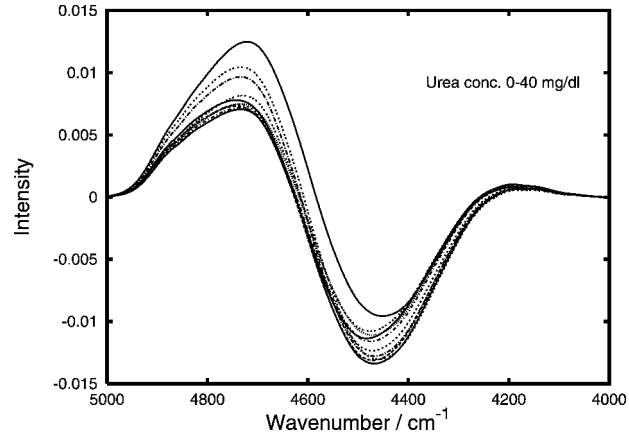

FIG. 3. Raw dual-beam spectra of urea measurements.

both inputs. If, in addition, the beam splitter is lossless such that $R = T = 0.5$ and $\Phi = \pi/2$, then the intensity at the detector is given by:

$$P_1 = 0.5(p_1 + p_2 + (p_1 - p_2)\cos\varphi) \qquad (2)$$

The measured dual-beam interferogram is the AC component of this quantity. It contains the difference between the two input sources. If the second input is zero, we have the usual expression for single-beam intensity at the detector:[26]

$$P_1 = 0.5p_1(1 + \cos\varphi) \qquad (3)$$

where, again, the measured interferogram is the AC component of this quantity. Note that the DC component in the single-beam expression, Eq. 3, is of the same order of magnitude as the AC component. In the dual-beam expression, Eq. 2, with p_1 and p_2 chosen to be nearly equal, the AC component is nearly zero but the DC component is twice as large as in the single-beam mode. This is the reason for the saturation of the MCT detector when used in the mid-IR for dual-beam spectroscopy.[11]

The absorbance spectrum is usually calculated from two single-beam spectra as $A = -\log_{10}(I/I_0)$; where I and I_0 are the sample and reference spectra. In the dual-beam mode of operation, one measures the difference between sample and reference $D = I - I_0$. Therefore, $I/I_0 = (D/I_0) + 1$ and $A \approx (1/\ln 10) \times (D/I_0)$ because D is much smaller than I_0. The measured dual-beam signal is seen to be proportional to the absorbance by a factor that depends on the reference intensity at a given wavenumber. The measured single-beam spectra are in principle not proportional to the absorbance, and it is common to take the log to linearize them. In our case, however, the variability of the measured single-beam spectra is very small and linearization has no effect other than giving a higher weight to the outer parts of the spectrum relative to the central part.

RESULTS AND DISCUSSION

Figure 2 shows the region around the center burst for typical interferograms measured through two identical cells containing pure water. The top interferogram (offset by 10 V) is measured in single-beam mode through the sample arm, and the middle interferogram is measured in single-beam mode through the reference arm. The bottom interferogram (offset by −4 V) is the combined dual-beam interferogram obtained with input from both the sample and reference arms. This dual-beam interferogram was measured at 15 times greater amplification than the two single-beam interferograms and was divided by this amplification factor for comparison with the single-beam interferograms. These interferograms demonstrate that the sample and reference signals are π out of phase and result in a nulled signal when combined. Achievable nulling ratios are in the range of 30 to 60, with the residual signal arising from a constant difference between the two input channels. Such interferograms are converted to intensity spectra as described in the Experimental section. Figure 3 shows the intensity spectra that make up the calibration set for dual-beam measurements of urea and Fig. 4 shows the corresponding intensity spectra for the single-beam measurements. The spectra in the dual-beam mode show much greater individual variation than the single-beam spectra, where the individual measurements are indistinguishable to the eye. The dual-beam measurement removes the variations that are common to both the reference and the sample, leaving only the difference between the two arms. In this way, the ADC is used to digitize only the signal of interest. Note that the intensity of a dual-beam spectrum may be negative owing to the use of the phase from a single-beam spectrum in constructing the dual-beam intensity spectra.

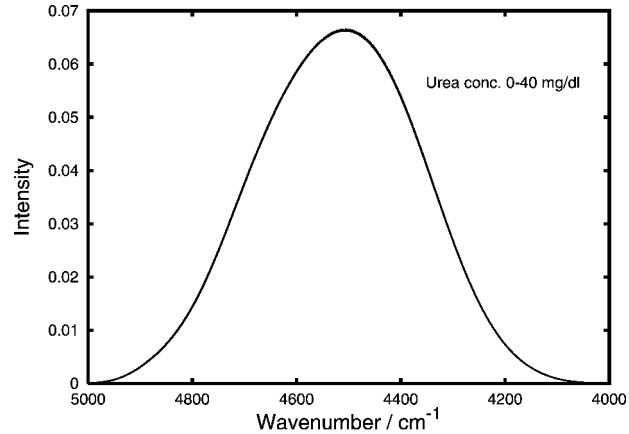

FIG. 4. Raw single-beam spectra of urea measurements.

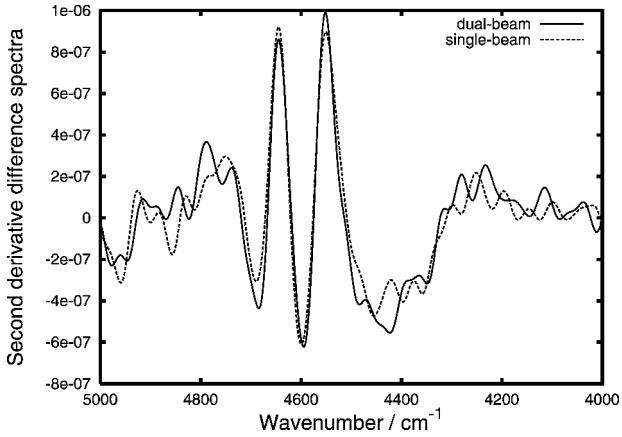

FIG. 5. Second derivative of raw dual- and single-beam difference spectra.

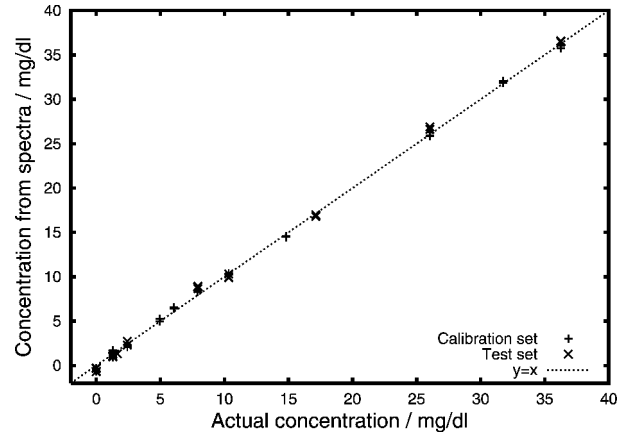

FIG. 7. Urea calibration from dual-beam data using four principal components.

To further illustrate any difference between the dual-beam and single-beam spectra, we chose a single-beam spectrum of a sample with a concentration of 36.26 mg/dL and subtracted a single-beam spectrum of a pure water sample. The second derivative of this spectrum was then calculated by finite three-point centered differencing. The same procedure was repeated for the corresponding dual-beam measurement. The single-beam data was multiplied by 15 to adjust for the higher amplification factor used in the dual-beam measurements. The result is shown in Fig. 5. Ideally, these two second-derivative difference spectra should be identical. Apart from noise, with a period corresponding to that of a spectrum that has not been zero-filled, this is the case. The spectrum of urea is clearly present in both and has the same magnitude. There is no visible effect of discretization present in the single-beam spectrum and no difference in noise level between the single-beam spectrum and the dual-beam spectrum.

Urea Calibration. Figure 6 shows the results of the PCR calibration on the dual- and single-beam data sets. The standard error of calibration and the standard error of prediction are plotted as a function of the number of principal components used in the calibration models for both dual-beam and single-beam data sets. The dual-beam calibration model needs only four principal components to successfully predict urea and yields similar rms error values for both calibration and test sets. No significant improvement is obtained by retaining more components. The single-beam calibration model, on the other hand, shows a lack of agreement between the calibration and test sets and needs nine principal components to give a standard error of calibration comparable to that obtained with the dual-beam data. The standard error of the test set is double that in the dual-beam calibration. Figures 7 and 8 show the calibration plots of the known vs. calculated concentrations for the four-factor calibration models based on dual- and single-beam data, respectively. The repeat measurements on the same samples also show a spread in the single-beam data that is not present in the dual-beam data, indicating that brief time variations in the instrument have been eliminated in the dual-beam measurement. Had these variations been caused by the sample, one would expect the repeat measurements in the dual-beam data sets to show a spread similar to that observed in the single-beam measurements. By increasing the number of principal components in the single-beam calibration model, the spread of repeat samples is much reduced. This result indicates that the spread of repeat samples is not primarily caused by higher noise content, but by some underlying instrumental variation, which may be modeled. This interpretation is supported by examination of the loading and regression

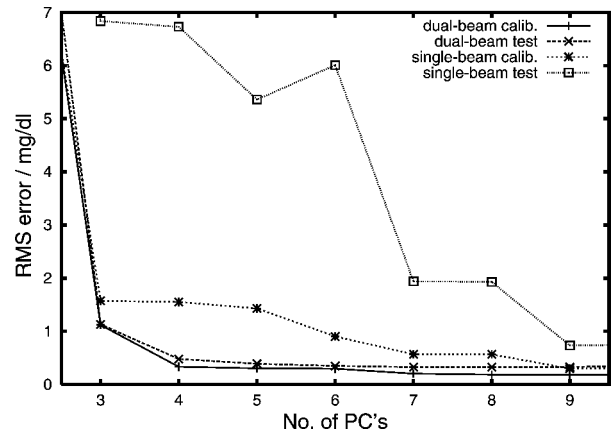

FIG. 6. Std. error of calibration/prediction for urea calibration based on single-beam and dual-beam data, respectively.

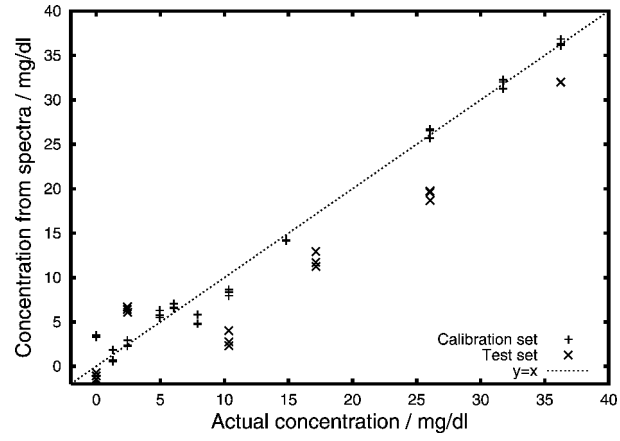

FIG. 8. Urea calibration from single-beam data using four principal components.

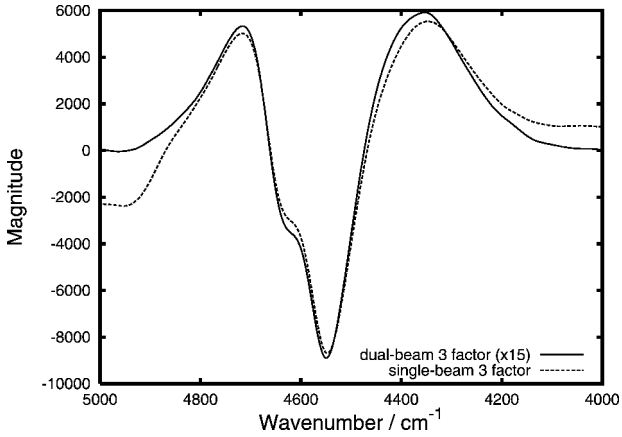

FIG. 9. Regression vectors for urea calibration, 3 principal components, dual-beam and single-beam.

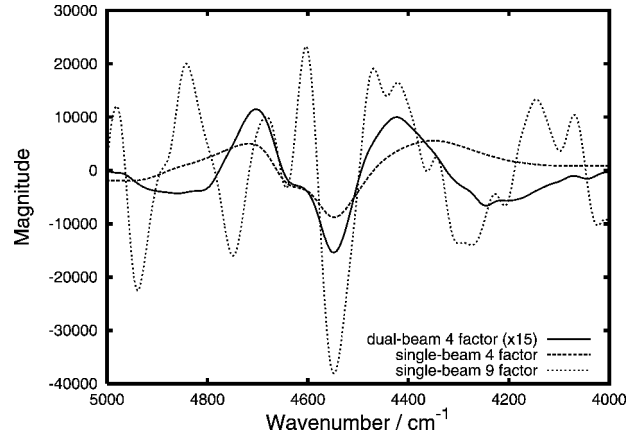

FIG. 10. Regression vectors for urea calibration, 4 principal components, dual-beam, and 4 and 9 principal components, single-beam.

vectors for the dual- and single-beam calibration models. In both models, the first two loading vectors describe variations in intensity, magnitude, and shift, and the third and fourth loading vectors carry information related to urea. The regression vectors obtained by using three principal components in the calibration models based on dual- and single-beam data, respectively, have nearly the same spectral structure. They differ in magnitude by a factor of 15, which was expected as the dual-beam interferograms have been amplified by this factor. Thus, the three most influential variations in the dual- and single-beam data sets are identical, as illustrated in Fig. 9, which shows the dual- and single-beam regression vectors for calibration models retaining three factors. The dual-beam regression vector has been multiplied by the amplification factor of 15. Other principal components in the two calibration sets do differ. The dual-beam data set does not contain any additional variations beyond the four principal components, but the single-beam data set contains at least five more that must be taken into account to obtain a usable calibration model. Inclusion of these additional principal components influences the regression vector such that it shows narrow features, not present in the spectrum of urea. These oscillations, with a period two times the spectral resolution, in the regression vector of the nine-factor single-beam calibration model could indicate that over-fitting has taken place. Yet the predictive ability of the concentrations in an independent data set is improved by using nine components. These findings are illustrated in Fig. 10, which shows the regression vectors with four principal components for the dual- and single-beam calibration models, and for the single-beam calibration model retaining nine principal components. The dual-beam regression vector has been multiplied by the amplification factor of 15.

Glucose Calibration. Carrying out the same analysis on the glucose data sets yielded similar results. Figure 11 shows the results of the PCR calibration on the dual- and single-beam data sets. The standard error of calibration and prediction is plotted as a function of the number of principal components used in the calibration for both dual- and single-beam data sets. Again, we find that four principal components are sufficient to model the solute in the dual-beam calibration model. The single-beam calibration model needs more factors and shows less agreement between the calibration and the test set. Again, the repeat measurements coincide in the four-factor calibration models based on dual-beam data but are spread out in the four-factor calibration model based on single-beam data (not shown). Dual- and single-beam regression vectors from four-factor models are similar, while single-beam regression vectors, based on more than four factors, contain narrow features that have no connection with the spectral structure of glucose (not shown). These narrow structures are similar to those present in the regression vector for urea based on nine factors. This seems to indicate that these structures are related to instrumental variations.

CONCLUSION

The results of both the urea and glucose calibrations indicate that the dual-beam measurements provide a day-to-day stability that the single-beam measurements do not and that variations caused by the instrument are greatly reduced. The dual-beam measurements thus provide better prediction with fewer principal components. We have not found any difference in discretization or noise level between the single- and dual-beam measurements. We believe that this is because sample variations dominate over the detector noise. We have demonstrated that the dual-beam technique provides superior data to that sup-

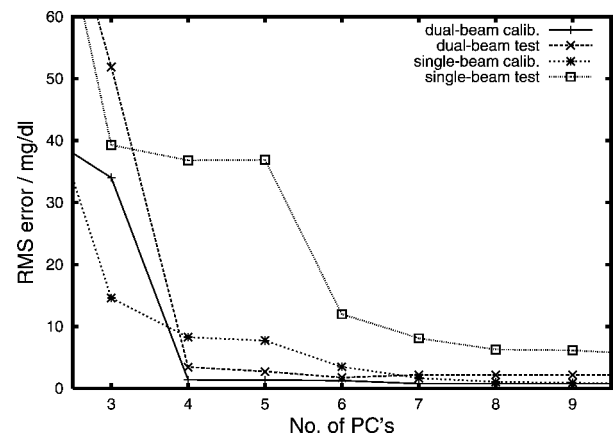

FIG. 11. Std. error of calibration/prediction for glucose calibration based on single-beam and dual-beam data, respectively.

plied by the single-beam technique. We have not investigated the effect of preprocessing the data to improve the calibration model. It seems likely that data preprocessing would improve the calibration model based on single-beam data more than the one based on dual-beam data, where variations have been removed in the measurement process. On the other hand, it is important to note that it is difficult to optimize the single-beam measurement, whereas the dual-beam measurement can be improved by increasing the intensity of the light source, and with it, the signal-to-noise ratio of the measurement. We expect that the simpler calibration models of the dual-beam technique will be important in measuring trace component concentrations in more complex fluids. We further hope that the elimination of instrumental effects in the measurement process will facilitate transfer of calibration from one instrument to another. The long-term stability of dual-beam measurements has not been investigated in this work. Clearly, the use of this technique in a commercial instrument requires that stable results be obtainable even when instrument parts, such as lamps, are replaced. For this purpose, it may be a challenge to obtain a reference spectrum, as is done in traditional spectroscopy, which does not introduce the defects of a single-beam measurement into the data.

ACKNOWLEDGMENTS

This work has been carried out under grant no. RK930.9750.0006.0035.0092.0 from the Danish Research Academy and has received financial support from the Danish Center for Biomedical Optics and New Laser Systems. Glucose measurements were carried out by Louise Brinck, Louise K. Mortensen, Louise R. Schmidt, Christian Schoenbeck, Klaus H. Gregersen, and Peter Madelung from Roskilde University.

1. V. H. Segtnan and T. Isaksson, J. Near. Infrared Spectrosc. **8,** 109 (2000).
2. A. R. Shaw, S. Kotowich, H. H. Mantsch, and M. Leroux, Clin. Biochem. **29,** 11 (1996).
3. R. Vonach, B. Lendl, and R. Kellner, Analyst (Cambridge, U.K.) **122,** 525 (1997).
4. R. Vonach, J. Buschmann, R. Falkowski, R. Schindler, B. Lendl, and R. Kellner, Appl. Spectrosc. **52,** 820 (1999).
5. T. Yano, T. Funatsu, K.-I. Suehara, and Y. Nakano, J. Near Infrared Spectrosc. **9,** 43 (2001).
6. C. V. Eddy and M. A. Arnold, Clin. Chem. **47,** 1279 (2001).
7. K. H. Hazen, M. A. Arnold, and G. W. Small, Appl. Spectrosc. **48,** 477 (1994).
8. K. H. Hazen, M. A. Arnold, and G. W. Small, Appl. Spectrosc. **52,** 1597 (1998).
9. K. H. Hazen, M. A. Arnold, and G. W. Small, Anal. Chem. Acta **371,** 255 (1998).
10. P. R. Griffiths and J. A. de Haseth, *Fourier Transform Infrared Spectrometry* (John Wiley and Sons, New York, 1986), pp. 98–311.
11. D. Kuehl and P. R. Griffiths, Anal. Chem. **50,** 418 (1978).
12. M. M. Gomez-Taylor and P. R. Griffiths, Anal. Chem. **59,** 422 (1978).
13. D. Kuehl, G. J. Kemeny, and P. R. Griffiths, Appl. Spectrosc. **34,** 222 (1980).
14. G. J. Kemeny and P. R. Griffiths, Appl. Spectrosc. **34,** 95 (1980).
15. D. L. Beduhn and R. L. White, Appl. Spectrosc. **40,** 628 (1986).
16. G. Laroche, J. Giroux, A. Bordeleau, and J. Garneau, Appl. Spectrosc. **48,** 356 (1994).
17. O. Shepard, W. Reidy, and G. A. Vanasse, Proc. SPIE-Int. Soc. Opt. Eng. **191,** 71 (1979).
18. T. Zehnpfennig, S. Rappaport, and G. A. Vanasse, Proc. SPIE-Int. Soc. Opt. Eng. **191,** 71 (1979).
19. C. P. Tripp and M. L. Hair, Langmuir **8,** 241 (1992).
20. C. P. Tripp and M. L. Hair, Appl. Spectrosc. **46,** 100 (1992).
21. E. L. Terpugov, A. V. Viskovatykh, O. V. Degtyareva, and E. E. Fesenko, Biophysics **43,** 954 (1998).
22. D. W. T. Griffith and B. Galle, Atmos. Environ. **34,** 1087 (2000).
23. W. H. Press, S. A. Teukolsky, W. T. Vetterling, and B. P. Flannery, *Numerical Recipes in C: The Art of Scientific Computing* (Cambridge University Press, Cambridge, 1995), 2nd ed.
24. M. Shane Hutson and M. S. Braiman, Appl. Spectrosc. **52,** 974 (1998).
25. L. Genzel, H. R. Chandrasekhar, and J. Kuhl, Opt. Commun. **18,** 381 (1976).
26. P. R. Griffiths and J. A. de Haseth, *Fourier Transform Infrared Spectrometry* (John Wiley and Sons, New York, 1986).